Rapid Formation of the Native 14-38 Disulfide Bond in the Early Stages of BPTI Folding†

Michal Dadlez‡ and Peter S. Kim*

Howard Hughes Medical Institute, Whitehead Institute for Biomedical Research, Department of Biology, Massachusetts Institute of Technology, Nine Cambridge Center, Cambridge, Massachusetts 02142

Received July 2, 1996; Revised Manuscript Received October 8, 1996⊗

ABSTRACT: Using recombinant variants of BPTI, we have determined the rate constants corresponding to formation of each of the fifteen possible disulfide bonds in BPTI, starting from the reduced, unfolded protein. The 14-38 disulfide forms faster than any of the other 14 possible disulfides. This faster rate results from significantly higher intrinsic chemical reactivities of Cys-14 and Cys-38, in addition to local structure in the reduced protein that facilitates formation of the 14-38 disulfide bond. This disulfide bond is found in native BPTI. Our results suggest that a significant flux of folding BPTI molecules proceed through the one-disulfide intermediate with the 14-38 disulfide bond, denoted [14-38], that has recently been detected on the BPTI folding pathway. In addition to providing a detailed picture of the early events in the folding of BPTI, our results address quantitatively the effect of local structure in the unfolded state on folding kinetics.

Bovine pancreatic trypsin inhibitor (BPTI)[1] is a small protein with three disulfide bonds between residues 5-55, 14-38, and 30-51 (Figure 1). When these disulfide bonds are reduced, the protein unfolds. The pathway of disulfide bond formation that accompanies the folding of BPTI has been studied for two decades (Creighton, 1974, 1977a; Creighton & Goldenberg, 1984; Weissman & Kim, 1991, 1992a,b, 1993, 1995; Goldenberg, 1992), but little is known about the earliest events in this folding reaction. Initially, the reduced protein (R) is oxidized to a large number of mixed-disulfide intermediates and, subsequently, to one-disulfide intermediates (Creighton, 1977b). It has recently been shown that an intermediate denoted [14-38], which contains a single disulfide bond between residues 14 and 38, dominates the spectrum of one-disulfide intermediates in the early stages of BPTI folding (Dadlez & Kim, 1995). At later stages, the one-disulfide species are known to rearrange at neutral pH predominantly to the intermediates denoted [30-51] and [5-55], each of which also contains a single native disulfide bond (Weissman & Kim, 1991).

BPTI contains six cysteines, so fifteen one-disulfide species are possible. A complete kinetic description of the initial events of BPTI folding requires measurement of the rates of formation for all of these species. Glutathione-mediated formation of an intramolecular disulfide bond proceeds in two steps. First (step 1 in Figure 2), a free thiol in the protein attacks the disulfide bond of oxidized glutathione (GSSG), releasing a molecule of reduced glutathione (GSH). This step yields a species with a disulfide bond between a protein Cys residue and a glutathione molecule, referred to as a mixed disulfide. In a second step (step 2 in Figure 2), a different protein thiol attacks the protein-glutathione mixed disulfide, resulting in the formation of a disulfide bond between two protein Cys residues and releasing a second molecule of GSH. Characterization of step 1 requires measurement of the rate constants of mixed-disulfide formation with glutathione for each of the six cysteine residues in BPTI. Characterization of step 2 requires measurement of the unimolecular rates of formation for each of the fifteen disulfide bonds that can form in BPTI. The protein disulfide bonds thus formed may then rearrange with free protein thiols in an intramolecular reaction.

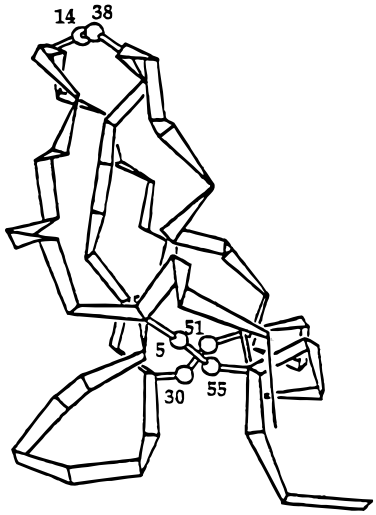

FIGURE 1: Schematic representation of the crystal structure of BPTI (Deisenhofer & Steigemann, 1975; Wlodawer et al., 1987), indicating the cysteine residues involved in disulfide bonds.

† This work was supported by the Howard Hughes Medical Institute.

‡ Current address: Institute of Biochemistry and Biophysics, Polish Academy of Sciences, ul. Pawinskiego 5A, 02−106 Warszawa, Poland.

⊗ Abstract published in *Advance ACS Abstracts,* November 15, 1996.

[1] Abbreviations: ANS, 1-anilino-8-naphthalenesulfonic acid; BPTI, bovine pancreatic trypsin inhibitor; C_{eff}, effective concentration of cysteines; DTNB, 5,5′-dithiobis(2-nitrobenzoic acid); GSH, reduced glutathione; GSSG, oxidized glutathione; HPLC, high-pressure liquid chromatography; IAc, iodoacetate; k_{bi}, rate constant for bimolecular disulfide rearrangement; k_{uni}, average rate constant for unimolecular disulfide rearrangement; $k^{x\rightarrow ySSz}$, rate constant for disulfide rearrangement with a free thiol *x* as a nucleophile, *y*S as a central sulfur, and S*z* as a leaving group; NOE, nuclear Overhauser effect; P*x*, a short peptide fragment of BPTI containing the cysteine corresponding to residue *x* in BPTI; TFA, trifluoroacetic acid; (*x*,*y*), a BPTI variant with cysteines at residues *x* and *y* and the remaining four cysteines replaced by alanines.

S0006-2960(96)01605-4 CCC: $12.00

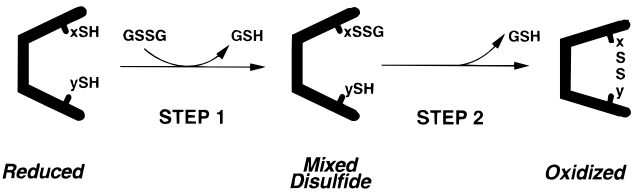

FIGURE 2: Formation of an intramolecular disulfide bond in a two-step reaction. In step 1, a free thiol in the protein attacks the disulfide bond of oxidized glutathione (GSSG). This step yields a species with a disulfide bond between a protein Cys residue and a glutathione molecule, referred to as a mixed disulfide. In step 2, a different protein thiol attacks the protein-glutathione mixed disulfide, resulting in the formation of a disulfide bond between two Cys residues in the protein.

Because the rate of disulfide rearrangement is proportional to the population of thiolate anions, the rearrangement rate is very slow at low pH. This strong pH dependence permits us to quench disulfide rearrangement by rapidly lowering the pH (Weissman & Kim, 1991), and to separate and purify the populated species chromatographically. After lyophilization, disulfide rearrangement may be resumed by redissolving the trapped, purified species in neutral pH buffer. This acid-quench method greatly facilitates the task of measuring the rates of disulfide rearrangement. The validity of using acid-quenching and high-pressure liquid chromatography (HPLC) analysis to study the folding of BPTI has been established (Weissman & Kim, 1991).

We have undertaken a systematic study of the rates of disulfide bond formation for each of the six cysteines in BPTI. Rate constants for mixed-disulfide formation (step 1 in Figure 2) were measured by reacting reduced BPTI protein mutants and peptide fragments with GSSG. Unimolecular rates of disulfide formation (k_{uni}; step 2 in Figure 2) were measured in 15 BPTI mutants, each corresponding to one cysteine pair. In each of these mutants, four different cysteines were replaced by alanines, leaving only two cysteines in their native positions. The mutants are denoted by indicating in parentheses the cysteines present: for example, (14,38) refers to the BPTI mutant containing cysteines at residues 14 and 38, with the other four cysteines replaced by alanine. The mixed-disulfide form of each mutant was purified by HPLC and then used to determine k_{uni}. Although some of the k_{uni} values have been estimated previously by indirect means, our studies provide direct, reliable measurements of k_{uni}.

Our results indicate that the rates of disulfide bond formation are influenced by both the intrinsic chemical reactivities of the cysteines and the conformational properties of the polypeptide chain linking the two cysteines. To determine the contribution from intrinsic chemical reactivities, the rates of both steps in Figure 2 were measured in a set of six peptides, fragments of BPTI, each containing one cysteine. To determine the effect of local structure in the polypeptide chain linking the two cysteines, C_{eff}, the effective concentration (Page & Jencks, 1971) of the cysteine residues, was measured for all fifteen possible cysteine pairs using BPTI mutants.

The C_{eff} values determined here correspond to kinetic effective concentrations, calculated for each pair of cysteines from two measured rate constants: k_{uni}, for formation of a disulfide between two cysteines in the intact polypeptide, and k_{bi}, for formation of a disulfide between these cysteines in two separate BPTI fragments. It is important to note the difference between the kinetic effective concentrations determined here and equilibrium effective concentrations (Creighton, 1983; Lin & Kim, 1989). An equilibrium effective concentration for two cysteines is a ratio of the unimolecular and bimolecular equilibrium constants for formation of the disulfide bond. Thus, interpretation of the equilibrium effective concentration is more difficult, since the value of C_{eff} depends on four, rather than two, rates of disulfide rearrangement. In particular, the rates of reduction of disulfides can vary substantially, especially for disulfide bonds that are strained or buried within a folded protein (Creighton & Goldenberg, 1984; Darby & Creighton, 1993; Goldenberg et al., 1993). In contrast, the kinetic C_{eff} measures the extent to which structure in the unfolded state brings two cysteines into proximity of each other. Thus, kinetic C_{eff} measurements are more appropriate as a means for probing structure in the reduced, unfolded state.

MATERIALS AND METHODS

General. Disulfide rearrangement experiments were performed in an anaerobic chamber (Coy Laboratory Products). All solvents were degassed, purged for 15 min with nitrogen, stirred in the anaerobic chamber for at least 24 h, and equilibrated at 25 °C prior to use. The level of residual oxidizing activity in these solvents was checked by incubating the reduced (14,38) BPTI mutant at pH 7.3 in the anaerobic chamber. No more than 2% of the starting material was found to undergo oxidation after incubation for 30 min, which is longer than the reaction time of the experiments presented here. The reactions were carried out in a circulating water bath in order to maintain a constant sample temperature of 25 °C. Reactants were first dissolved in H_2O (containing glutathione or urea or both where necessary) acidified to pH 3 with HCl. A small aliquot was withdrawn from the low-pH sample and analyzed by HPLC in order to obtain the elution profile for disulfide rearrangement at time zero. Disulfide rearrangement was initiated by adding to the remainder of the starting mixture (with vigorous stirring) $^1/_4$ volume of 0.5 M phosphate buffer, 1 M NaCl, 5 mM EDTA, to give final conditions of 0.1 M phosphate buffer, pH 7.3, 0.2 M NaCl, 1 mM EDTA. For analytical reactions, the final protein concentration was 5−10 μM. At the appropriate times, aliquots of the refolding mixture were quenched to a final pH of ~2 by addition of $^1/_{20}$ volume of formic acid (or HCl in the case of urea-containing samples). The quenched samples were transferred to an automatic sample injector, where they were cooled to 4 °C and then analyzed by HPLC. The order in which the samples were injected was altered in order to check the efficiency of acid quenching [see Weissman and Kim (1991)]. The pH of the remaining, unquenched portion of the folding reaction was checked at the end of each experiment. Urea was prepared fresh on a daily basis. Samples containing urea were desalted or diluted prior to HPLC analysis.

Reversed-phase HPLC was performed using Vydac C-18 columns immersed in a water bath heated to 35 °C. A linear gradient of solvent A (0.1% TFA in H_2O) and solvent B (90% vol/vol acetonitrile in H_2O, 0.1% TFA) was used. Absorbance was monitored at both 229 and 280 nm. The peak areas were calculated using the Dynamax (Rainin Instruments) HPLC data analysis program. Purified samples were lyophilized and stored desiccated at low temperature.

Species were assigned according to their molecular masses. Laser desorption mass spectrometry was performed with a

Finnigan MAT Lasermat. Samples were mixed with matrix (α-cyano-4-hydroxycinnamic acid) in 70% acetonitrile, 30% H_2O, 0.1% TFA.

Expression and Purification of BPTI Mutants. The BPTI mutants were expressed as fusion proteins in *Escherichia coli* strain BL21 (DE3) pLysS, using the T7 system (Studier et al., 1990), as described previously (Staley, 1993; Staley & Kim, 1994). Briefly, the pAED4 plasmids (Doering, 1992) encoding a portion of the trpΔLE 1413 polypeptide (serving as a leader sequence) followed by a Met residue and the BPTI mutant gene, were prepared by oligonucleotide-directed mutagenesis (Kunkel et al., 1987). The gene sequence was confirmed for each mutant by dideoxynucleotide sequencing. Transformed cells were grown from overnight cultures in Luria broth (100 μg/mL ampicillin, 30 μg/mL chloramphenicol) to $A_{590} = 1$. Cells were induced with 0.4 mM isopropyl β-D-thiogalactopyranoside (IPTG) and harvested after 2.5 h by centrifugation. Cells were lysed by freezing, followed by sonication in 50 mM Tris, pH 8.7, 15% glycerol, 100 μM $MgCl_2$, 10 μM $MnCl_2$, 10 μg/mL DNAse I. After centrifugation, the pellet was resuspended in 50 mM Tris, pH 8.7, 1% Nonidet (NP40), 1% deoxycholic acid, 1 mM EDTA, and then sonicated and centrifuged. Finally, the pellet was dissolved in 6 M GuHCl, 50 mM Tris, pH 8.7, 10 mM GSSG, and then sonicated and incubated at room temperature for 15 min. The resulting mixture was divided into 5 mL fractions, and each fraction was diluted 10-fold with H_2O and then centrifuged. The pellet was resuspended in 70% formic acid, and ∼200 mg of cyanogen bromide was added to initiate cleavage. After 2.5 h, the mixture was centrifuged under vacuum for 4 h, diluted 10-fold with H_2O, dialyzed against 5% acetic acid, and lyophilized. The sample was redissolved in 6 M GuHCl, 0.1 M dithiothreitol (DTT), 0.1 M Tris, pH 8.7, and dialyzed again against 5% acetic acid. The dialysate was centrifuged and filtered prior to purification on a Vydac C-18 preparative HPLC column. The molecular mass of the collected material, as determined by laser desorption mass spectroscopy, was always 6372 ± 2, as expected.

Substitution of cysteines in BPTI by alanines has been shown previously to be least disruptive of native structure (Staley & Kim, 1992; Marks et al., 1987; Hurle et al., 1992). It has also been shown that an additional substitution, M52L, introduced in our series of mutants, has no effect on BPTI stability (Yu et al., 1995), and is sometimes encountered in homologous proteins (Creighton & Charles, 1987).

Peptide Synthesis. Peptides were synthesized using solid phase *t*-Boc methods, as described previously (Goodman & Kim, 1989). Peptides were desalted on a G-10 column and purified to homogeneity by HPLC. The peptides are denoted by a capital P, followed by the cysteine residue that is being modeled: for example, P14 corresponds to the peptide used to model the local environment of Cys-14. Peptide sequences were as follows: P5 (RPDF**C**LEPPY-$CONH_2$); P14 (Ac-PYTGP**C**KAR-$CONH_2$); P30 (YNAKAGL**C**QTF-$CONH_2$); P38 (Ac-YGG**C**RAKRNN-$CONH_2$); P51 (Ac-YKSAED**C**LRT-$CONH_2$); P55 (Ac-YKSAEDALRT**C**G-GA). These peptides correspond to fragments of BPTI M52L, with the sequence RPDF$\mathbf{C}^{5}$LEPPYTGP$\mathbf{C}^{14}$-KARIIRYFYNAKAGL$\mathbf{C}^{30}$QTFVYGG$\mathbf{C}^{38}$RAKRNN-FKSAED$\mathbf{C}^{51}$LRT$\mathbf{C}^{55}$GGA. Cysteines and their positions in the native BPTI sequence are highlighted. In peptides P51 and P55, tyrosine was introduced in place of the native residue phenylalanine 45 to facilitate determination of peptide concentration. Also in peptide P55, the cysteine at position 51 in native BPTI was replaced by alanine. Each peptide contains at least three native residues preceding and following the cysteine in the native BPTI sequence.

Concentration Measurements. Concentrations of all reactants were determined by measuring HPLC peak areas as follows. First, the response of the HPLC UV detector to the elution of a known amount of each species was measured. The response factor (Chau & Nelson, 1991) linking the sample amount injected with the peak area observed, both at 229 and 280 nm, was determined by repeated HPLC analysis of aliquots of standard samples, for which the concentration had been measured by other methods. An automatic HPLC sample injector (Waters WISP 717) was used, ensuring a high degree of reproducibility in the sample amount injected. For BPTI protein mutants, standard sample concentrations were measured spectroscopically, assuming an extinction coefficient of 5720 M^{-1} cm^{-1} at 275 nm (Kosen et al., 1981). For peptide fragments and reduced glutathione, standard sample concentrations were measured using 5,5′-dithiobis(2-nitrobenzoic acid) (DTNB), and an extinction coefficient of 14 150 M^{-1} cm^{-1} for the 2-nitro-5-thiobenzoate dianion at 412 nm (Riddles et al., 1979). The concentration of oxidized glutathione in the standard sample was determined by measuring the absorbance at 248 nm, using an extinction coefficient of 382 M^{-1} cm^{-1} (Huyghues-Despointes & Nelson, 1990). The response factors obtained for reduced and oxidized glutathione agree well with those measured previously (Chau & Nelson, 1991). To determine the concentrations of oxidized and reduced glutathione in the samples, small aliquots of each sample were withdrawn and injected onto an HPLC column equilibrated in 100% solvent A at room temperature and eluted isocratically, so that reduced and oxidized glutathione could be separated. Absorbance was monitored at 229 nm.

Formation of a disulfide bond introduces additional absorption bands in the UV spectra of the mutants and peptide fragments, but these bands are much weaker than the strong absorption bands of both the tyrosines at 280 nm and the tyrosines plus the peptide bonds at 229 nm (Donovan, 1969). Accordingly, we assume here that formation of a disulfide bond does not change the HPLC detector response factors measured for peptides and proteins in the reduced state.

Isolation of Single Mixed-Disulfide Species. The reduced form of each BPTI mutant was reacted with oxidized glutathione (GSSG) to obtain the mixed disulfides with glutathione. Five species are expected to result from this reaction [the reduced form, two single mixed disulfides, one double mixed disulfide, and the intramolecularly oxidized species (Figure 3a,b)]. In nine of the fifteen mutants, both single mixed-disulfide species could be isolated as separate peaks by HPLC. The single mixed disulfides were prepared as follows. First, 2−3 mg of reduced protein mutant were dissolved in 0.2 mL of 6 M GuHCl, 0.1 M acetate buffer, pH 4, and added to 2 mL of 0.1 M oxidized glutathione, 6 M GuHCl, 0.1 M phosphate buffer, pH 7.3, 1 mM EDTA, with vigorous stirring and purging with N_2 at room temperature. After 0.5−2 min, reactions were quenched with $^1/_{20}$ volume of HCl and desalted on a PD-10 (Pharmacia) G-25 column. The species were purified by HPLC, using a gradient of 31−35% solvent B in 80 min.

For the (14,30), (38,51), and (38,55) mutants, both single mixed disulfides coeluted; for the (30,51) and (5,30) mutants,

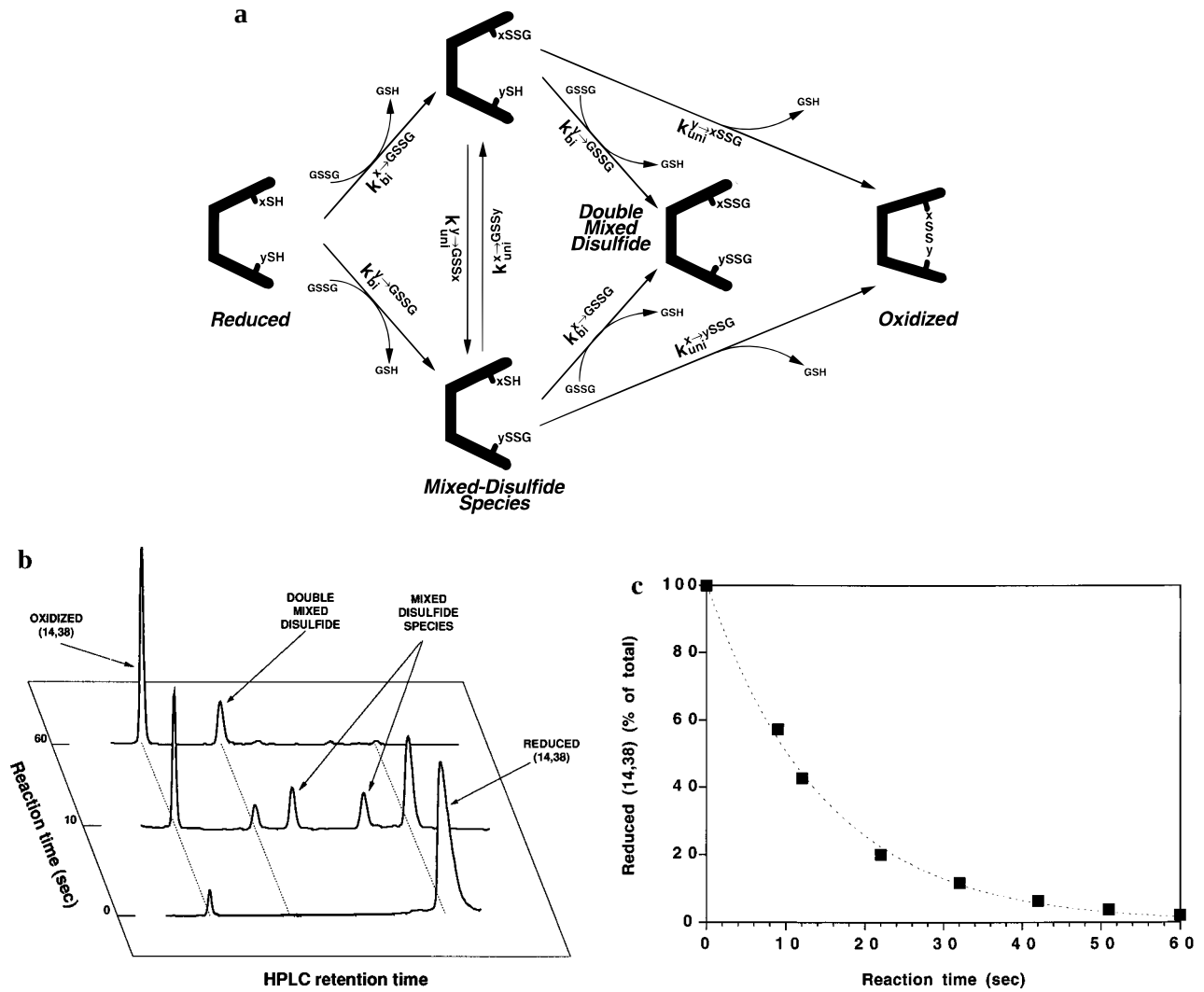

FIGURE 3: Measurement of reaction rate constants of protein thiols with oxidized glutathione. (a) Schematic of the reaction of a protein mutant containing two cysteines with oxidized glutathione. The reduced BPTI mutant, dissolved in neutral-pH buffer containing an excess of GSSG, undergoes oxidation, first to the mixed-disulfide species, then to either the unimolecularly oxidized or the double mixed-disulfide species. The amount of reduced glutathione that is produced is very small, so the reverse process (protein disulfide reduction) is not taken into account. (b) Reaction of reduced (14,38) with oxidized glutathione (5mM GSSG, pH 7.3, 25 °C). Chromatograms for aliquots taken at 0, 10, and 60 s are shown, along with peak assignments. Absorbance is monitored at 229 nm. Peaks were assigned based on molecular masses as follows: reduced (14,38) (molecular mass measured/expected: 6372/6372); mixed disulfide (14,38) with glutathione attached to either the first or the second cysteine (6677/6677, 6678/6677); double mixed disulfide (14,38) with glutathione molecules on both cysteines (6985/6982); oxidized (14,38) (6372/6370). A small peak corresponding to the oxidized species (as observed in the 0 s time point) results from a minor amount of oxidation of the reduced protein sample. (c) Decrease in the population of reduced (14,38) with time (filled squares). The peak areas for the reduced species are shown as a % of the sum of peak areas for the oxidized, single, and double mixed-disulfide species. The sum of these peak areas did not change significantly during the experiment (data not shown). The sum of the rate constants for the reaction between each cysteine and glutathione is obtained from the best fit of a monoexponential decay to the data (line).

the unimolecularly oxidized species coeluted with one of the mixed disulfides; for the (51,55) mutant, all three species coeluted. In these cases, the peaks containing mixtures of these different species were collected and used for rate measurements, as described below.

A similar procedure was used to prepare mixed-disulfide species from the BPTI peptide fragments containing one cysteine, using lower glutathione concentrations (50 mM) and longer reaction times (up to 10 min), but without the additional quenching and desalting steps, and an HPLC gradient of 0.5% solvent B per minute.

Reactivity of Peptide and Protein Thiols toward Glutathione and Iodoacetate. In order to measure the reactivities of the various protein thiols, reduced protein mutants were reacted with 5 mM GSSG. During this reaction, the reduced protein undergoes oxidation, first to the mixed-disulfide species with glutathione and then to either an intramolecularly oxidized species or a double mixed disulfide with glutathione (Figure 3a,b). Aliquots of the reaction mixture, quenched at different time points, were analyzed by HPLC, using a gradient of 30−34% solvent B in 40 min. 20 μL of the unquenched portion of the sample was used to determine the concentration of glutathione.

Because the sample contains an excess of GSSG, the formation of mixed disulfides is a pseudo-first-order reaction. Thus, the population of reduced protein molecules decays monoexponentially, with the rate constant equal to

$$k_{obs} = (k_{bi}^{x\rightarrow GSSG} + k_{bi}^{y\rightarrow GSSG}) \times [GSSG] \times 2 \qquad (1)$$

where $k_{bi}^{x\rightarrow GSSG}$ and $k_{bi}^{y\rightarrow GSSG}$ are the rate constants for the formation of mixed disulfides between glutathione and protein cysteines x and y, respectively, [GSSG] is the concentration of oxidized glutathione, and the factor of 2

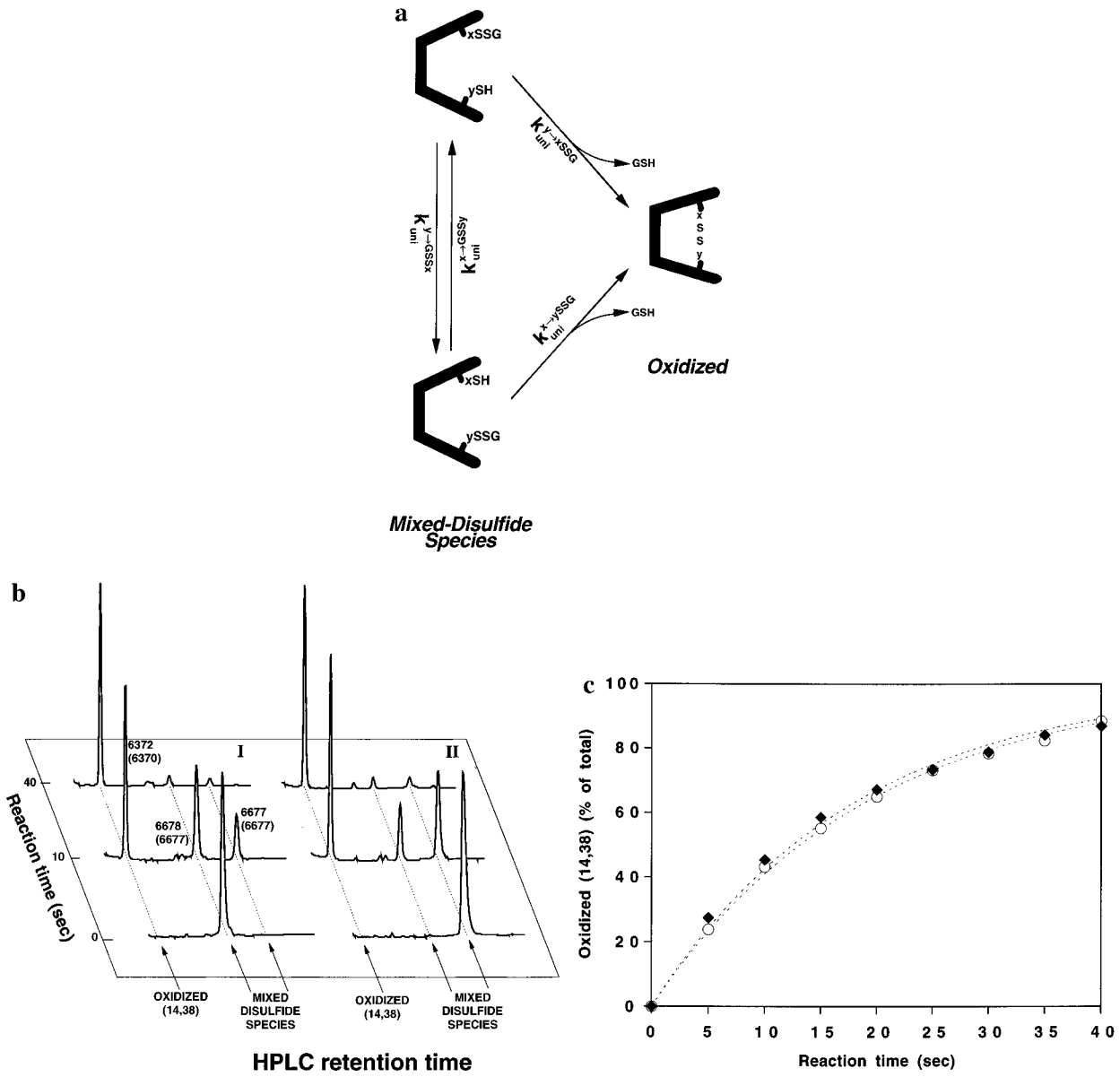

FIGURE 4: Measurements of k_{uni}. (a) Schematic for the rearrangement of a mixed-disulfide species to oxidized protein. Since the reaction starts with a mixed-disulfide species (*x*SSG or *y*SSG), no external oxidizing agent is needed, and the unimolecular rate of oxidation (k_{uni}) can be measured directly from the rate of build-up of the population of oxidized molecules. (b) HPLC chromatograms taken during two separate mixed-disulfide rearrangement experiments with the (14,38) mutant, monitored at 229 nm (pH 7.3, 25 °C). Chromatograms at three time points (0, 10, and 40 s) are shown, along with peak assignments. Peak identities were assigned according to molecular masses. Measured and expected (in parentheses) masses are shown. Experiments in lanes I and II start with a purified single mixed-disulfide species in which a glutathione molecule is attached to one of the two cysteines in the sequence. (c) The increase in the population of oxidized species over time was monitored in two separate rearrangement experiments, starting with each of the two single mixed-disulfide species of (14,38) (circles and diamonds). Peak areas for the oxidized species are shown as a percent of the sum of peak areas for the oxidized and the mixed-disulfide species. The best fit to eq 4 for both experiments is shown (dotted lines). The sum of the peak areas for the oxidized and mixed-disulfide species does not change during the experiment by more than 10% (data not shown).

accounts for the two sulfurs in GSSG (Creighton, 1986). Although this reaction results in the formation of reduced glutathione (GSH), its concentration is always so low as to be negligible. k_{obs} (and thus the sum of the rate constants for the formation of mixed disulfides between glutathione and cysteines *x* and *y*) was obtained (Figure 3c) by fitting the equation of a monoexponential decay to the observed decay of the population of the reduced species.

The decay of the reduced form of each peptide fragment was used, in a similar fashion, to calculate the rate constants for the reaction of each peptide fragment with glutathione. The mixed-disulfide forms of all peptides studied here elute faster from a C-18 HPLC column than do their reduced forms. The monoexponential decay curve was fit to these data to obtain k^{GSSG}, the rate constant for reaction of the cysteine residue with glutathione.

For the majority of peptides, however, blocking of thiols by IAc did not alter the HPLC retention times significantly. In these cases, k^{IAc}, the rate constant for reaction of the cysteine residue with iodoacetate, was determined by quenching the IAc reaction at different reaction times using 0.2 M GSSG instead of acid. Addition of the high concentration of GSSG converted unreacted peptide molecules to mixed disulfides with glutathione. Mixed disulfides with GSSG elute faster than do molecules that are reduced or blocked with IAc. Again, the reacted and unreacted populations at each reaction time were measured and k^{IAc} calculated. The efficiency of GSSG quenching was checked using the

peptides for which IAc blocking shifted the HPLC retention time; both quenching methods gave similar results. Peptide concentration was 50 μM, GSSG concentration for k^{GSSG} measurements was 5 mM, and IAc concentration was 10 mM.

Measurements of k_{uni}. Average rate constants for unimolecular disulfide formation in the protein mutants were measured by following the rearrangement of single mixed-disulfide species to oxidized species (Figure 4). Mixed-disulfide species were incubated at pH 7.3 for different times, in the absence of external oxidizing or reducing agents, and acid-quenched aliquots of the reaction samples were analyzed by HPLC. The gradient was 30−34% solvent B in 40 min. From the resulting elution profiles, the peak areas and the concentrations of all three species accumulating during the course of the reaction (both mixed disulfides and the intramolecularly oxidized species) were measured. The increase in peak area for the oxidized species, [OXI](t), relative to total species, was monitored (Figure 4c). The sum of the three peak areas does not change by more than 10% during a typical experiment.

The differential equation

$$d[OXI](t)/dt = k_{uni}^{x\rightarrow ySSG}[ySSG](t) + k_{uni}^{y\rightarrow xSSG}[xSSG](t) \quad (2)$$

describes the increase in the population of oxidized species as a function of time, where $k_{uni}^{x\rightarrow ySSG}$ and $k_{uni}^{y\rightarrow xSSG}$ represent the rate constants for formation of the disulfide bond in a unimolecular reaction between thiol x and the mixed disulfide with cysteine y or between thiol y and the mixed disulfide with cysteine x, respectively. [ySSG](t) and [xSSG](t) denote the populations of mixed disulfides with cysteines y and x, respectively. Again, the amount of reduced glutathione formed as a result of this reaction is negligible for these measurements.

It is usually assumed (Creighton, 1986) that $k_{uni}^{x\rightarrow ySSG}$ and $k_{uni}^{y\rightarrow xSSG}$ have similar values (see also below), so that these terms may be substituted by their average (k_{uni}) and the equilibrium between the mixed-disulfide species can be ignored. Accordingly, eq **2** simplifies to

$$d[OXI](t)/dt = k_{uni}([xSSG](t) + [ySSG](t)) = k_{uni}(1 - [OXI](t)) \quad (3)$$

This equation has a solution in the form of a monoexponential build-up of oxidized species, since [OXI](0) = 0:

$$[OXI](t) = 1 - \exp(-k_{uni}t) \quad (4)$$

This simplified equation was used to obtain k_{uni} from a single-parameter fit of eq 4 to the build-up curve for the oxidized species (Figure 4c). Repeated measurements of k_{uni} in mutants (5,55), (5,51), (14,30), and (14,38) gave values reproducible within ±10%.

k_{bi} Measurements. Bimolecular disulfide exchange rates were measured by following the disulfide rearrangement between two peptides (Figure 5). For these experiments, a peptide (50−100 μM) in reduced form (Px) was incubated with an excess concentration (0.5−1 mM) of the mixed-disulfide form of a different peptide (PySSG). In the course of the disulfide exchange, seven species (two reduced peptides, two mixed disulfides, two homodimers, and a heterodimer) are expected to form. Each individual peptide contains a single tyrosine residue. The peak areas at 280 nm of all species were measured from the HPLC elution profiles of aliquots of the reaction mixture, quenched at different times. The extinction coefficient for PxSSPy at 280 nm is assumed to be the sum of the extinction coefficients for the two peptides. The concentration of oxidant (PySSG) was also monitored by its peak area at 280 nm and found not to change significantly during the experiment. For these experiments, a semi-preparative HPLC column was used with a gradient of 5−35% solvent B in 60 min.

Three of the species populated during the experiment contain peptide Px (Figure 5a,b): the reduced form, the mixed disulfide with glutathione, and peptide Px disulfide bonded to peptide Py. The population of PxSSPx homodimer is always low, so its presence is not taken into account. When the mixed disulfide PySSG is in excess, oxidation of reduced peptide Px is a pseudo-first-order reaction. Thus, the population of Px decays as a single exponential:

$$[Px](t) = \exp(-k_{obs}[PySSG]t) \quad (5)$$

where k_{obs} is the sum of the two bimolecular rate constants $k_{bi}^{x\rightarrow ySSG}$ and $k_{bi}^{x\rightarrow GSSy}$ (Figure 5a), with the central sulfur (Szajewski & Whitesides, 1980) coming either from peptide Py or from glutathione, respectively. Of interest is the first rate constant ($k_{bi}^{x\rightarrow ySSG}$), which describes the bimolecular formation of a disulfide bond between the two peptides (PxSSPy). With excess mixed-disulfide species, the concentration of free thiols is relatively low, so the build-up of the PxSSPy population follows the equation

$$d[PxSSPy](t)/dt = k_{bi}^{x\rightarrow ySSG}[PySSG][Px](t) \quad (6)$$

Taking eq 5, [PxSSPy](0) = 0, and integrating, we get

$$[PxSSPy](t) = (k_{bi}^{x\rightarrow ySSG}/k_{obs})(1 - \exp(-k_{obs}[PySSG]t)) \quad (7)$$

where [PySSG] is an excess concentration of a mixed disulfide with peptide Py, measured by its peak area and constant during the experiment, and k_{obs} is obtained from a single-parameter fit of eq 5 to the decay of the population of reduced species [Px](t), measured during the same experiment. Thus, a single-parameter fit of [PxSSPy](t) to eq 7 gives the value of $k_{bi}^{x\rightarrow ySSG}$ (Figure 5c).

RESULTS

To facilitate comparison with earlier studies on the folding of BPTI (Weissman & Kim, 1991, 1992a,b, 1993, 1995; Dadlez & Kim, 1995), the experiments were carried out at 25 °C, 0.1 M Tris buffer, pH 7.3, 0.2 M NaCl, 1 mM EDTA, unless stated otherwise.

Step 1: Rates of Formation of Mixed-Disulfide Species. The first step in the formation of an intramolecular disulfide bond is the formation of a mixed disulfide (Figure 2). The rate constants for the reaction of oxidized glutathione (GSSG) with a set of six peptides, corresponding to fragments of BPTI (Table 1) and a set of fifteen BPTI mutants (Figure 3 and Table 2, column 2), were measured. Each mutant contains two of the six cysteines in BPTI, with the remaining four cysteines replaced by alanines. There is a notable (up to 7-fold) difference in the rates at which these mutants react with GSSG. This difference can result from either different intrinsic reactivities of the cysteines, or structural features

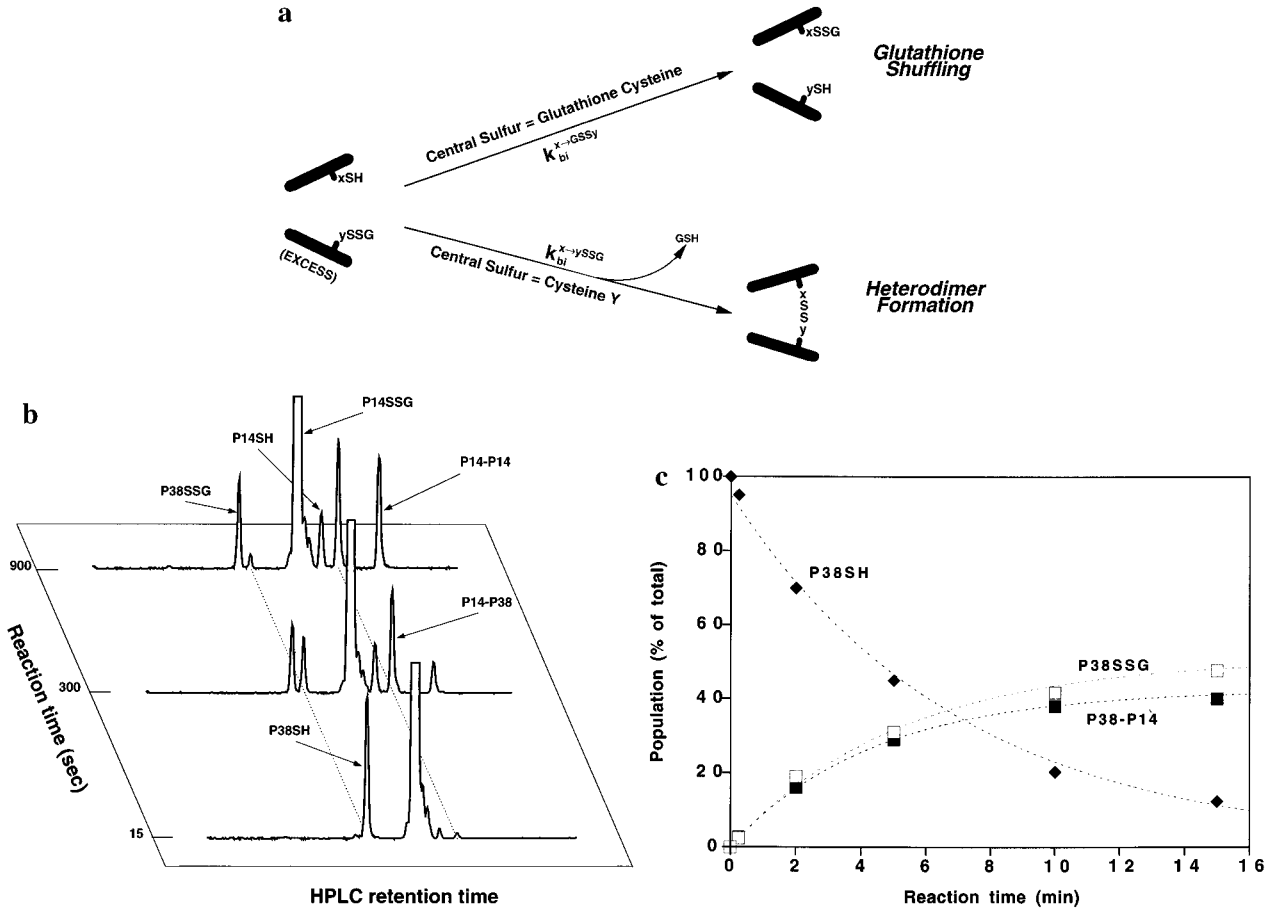

FIGURE 5: Measurements of k_{bi}. (a) Schematic for bimolecular disulfide rearrangement. When the reduced form of one peptide (P*x*) is mixed in a neutral-pH buffer with an excess of the mixed-disulfide form of a second peptide (P*y*SSG), two new species containing peptide P*x* are formed: disulfide bonded to glutathione (P*x*SSG) and disulfide bonded to peptide *y* (P*x*SSP*y*). In the pseudo-first-order conditions of excess mixed-disulfide species, the two species do not undergo further rearrangements. In both reactions, the same three thiol groups are involved, but the glutathione and peptide *y* thiol serve as either a central sulfur or a leaving group (Szajewski & Whitesides, 1980). In the first process, called "glutathione shuffling", a nucleophilic thiol of peptide *x* forms a mixed disulfide with glutathione, releasing reduced peptide *y*. In the second process, a heterodimer is formed between peptides *x* and *y*, and reduced glutathione is released. The build-up of the P*x*SSP*y* species allows for direct measurement of k_{bi} for the reaction of thiol *x* and mixed disulfide *y*SSG ($k_{bi}^{x\rightarrow ySSG}$), as described in Materials and Methods. (b) Chromatograms taken during bimolecular disulfide rearrangement experiments with reduced peptide P38 and an excess of the mixed disulfide of peptide P14 (P14SSG). Chromatograms monitored at 280 nm are shown for three time points (15, 300, and 900 s). Peaks are assigned based on their molecular masses as follows: P38SSG, mixed disulfide with P38 (molecular mass measured/expected: 1486/1485); P38SH, reduced P38 (1181/1180); P14SSG, mixed disulfide with P14 (1339/1339); P14SH, reduced P14 (1034/1034); P14-P38, peptide P14 disulfide bonded to P38 (2213/2212); P14-P14, peptide P14 disulfide-bonded dimer (2066/2066). (c) Population changes in reduced P38 (diamonds), P38-P14 (filled squares), and P38SSG (open squares) during the reaction of reduced P38 with an excess of P14SSG. The summed concentrations of different forms of peptide P38 did not change significantly during the experiment, as judged by the sum of their HPLC peak areas (data not shown). Best fits to eqs 5 and 7 (dotted lines) are shown.

Table 1: Second-Order Rate Constants for the Reaction of Cysteines with Glutathione (GSSG) and Iodoacetate (IAc) in Peptide Fragments of BPTI[a]

cysteine number	k^{IAc}		k^{GSSG}		k^{GSSG} (8 M urea)	
	(M^{-1} s^{-1})	normalized	(M^{-1} s^{-1})	normalized	(M^{-1} s^{-1})	normalized
5	0.1	[0.2]	0.3	[0.3]	0.06	[0.3]
14	0.9	[1.8]	2.4	[2.0]	0.45	[1.9]
30	0.5	[1.0]	0.9	[0.8]	0.2	[0.8]
38	0.9	[1.8]	2.4	[2.0]	0.5	[2.1]
51	0.2	[0.4]	0.4	[0.3]	0.08	[0.3]
55	0.4	[0.8]	0.8	[0.7]	0.15	[0.6]

[a] Numbers in square brackets are the values normalized to the average for a given column. Reactions were performed at 25 °C, pH 7.3, 0.1 M phosphate buffer, 0.2 M NaCl, 1 mM EDTA.

of the polypeptide chain that decrease the accessibility of the cysteines to different extents.

To measure the intrinsic reactivities of the different cysteines, the rate constants for reaction with GSSG were measured in a set of peptides, fragments of BPTI containing one cysteine each (Table 1). Again, a significant variability among rates is observed. Moreover, the rate constants calculated for the protein mutants from the rate constants measured in the peptide fragments, by assuming simple additivity, match closely the rate constants measured directly in the protein mutants (Table 2). This correlation indicates that the variability in the rates of reaction with GSSG in the protein mutants is a local effect (i.e., dependent on intrinsic reactivities), and that the global structure of reduced BPTI

Table 2: Reactivities of Cysteine Residues in BPTI Variants

BPTI mutant: cysteine positions	k^{GSSG} (M^{-1} s^{-1}) measured	k^{GSSG} (M^{-1} s^{-1}) predicted from reactivities in fragments[a]
5,14	2.9	2.7
5,30	1.3	1.2
5,38	2.7	2.7
5,51	0.7	0.7
5,55	1.1	1.1
14,30	3.2	3.3
14,38	4.9	4.8
14,51	2.8	2.8
14,55	3.2	3.2
30,38	3.5	3.3
30,51	1.4	1.3
30,55	1.7	1.7
38,51	2.8	2.8
38,55	3.3	3.2
51,55	1.3	1.2
14,30 (8 M urea)	0.5	0.6
14,38 (8 M urea)	0.9	1.0

[a] The sum of reaction rate constants of appropriate cysteines taken from Table 1.

does not affect the accessibility of cysteines significantly.

The reactivity of each cysteine was also measured in reactions with iodoacetate (IAc) and with GSSG in 8 M urea (Tables 1 and 2). The relative reactivities of the cysteines ("normalized" values in Table 1) are very similar in the presence or absence of urea and when GSSG is compared to iodoacetate. Taken together, these results indicate clearly that different cysteine residues in BPTI have significantly different intrinsic reactivities as nucleophiles, and that these differences are determined predominantly by the chemical nature of the residues in the immediate vicinity of the cysteine residues.

Step 2: Rates of Intramolecular Rearrangement. The second step in formation of an intramolecular disulfide bond is rearrangement of the mixed-disulfide species to form a disulfide bond between two protein Cys residues. To obtain the disulfide rearrangement rates, reversibly trapped (acid-quenched) mixed-disulfide species were prepared and purified by HPLC for each of the protein mutants. When redissolved in neutral pH buffer, these protein mixed disulfides rearrange spontaneously, in the absence of external oxidizing agents, to form unimolecularly oxidized species, according to the scheme shown in Figure 4a. These experiments (Figure 4) allow us to determine k_{uni} (Table 3) directly, without assumptions about intrinsic reactivities, as described in Materials and Methods. No reduced or double mixed-disulfide species were observed during these experiments, indicating that the disulfide rearrangement was unimolecular.

For nine of the fifteen mutants, it was possible to isolate each of the single mixed-disulfide forms. The rates of forming oxidized species starting from either form did not differ by more than 30%. This indicates that the simplification used in eq 3 is justified. The final value of k_{uni} is the average of at least two sets of experiments.

For the (14,30), (38,51), and (38,55) mutants, the two mixed-disulfide forms elute simultaneously from the HPLC column, and only a mixture containing both mixed-disulfide forms could be isolated. This mixture was used as the starting material for the disulfide rearrangement experiment. Because the oxidized forms of these three mutants elute earlier from the HPLC column than do the mixed-disulfide forms, the relative populations of these species could be measured for different reaction times and k_{uni} obtained.

For the (51,55) mutant, both mixed-disulfide forms and the oxidized form have similar retention times. Here again the mixture was isolated, but in this case the disulfide rearrangement was quenched with a high concentration (0.2 M) of GSSG instead of acid. This converts all single mixed disulfides to double mixed disulfides, which elute earlier from the HPLC column than the oxidized species. This method allowed us to separate the oxidized and mixed-disulfide species for each reaction time and to measure k_{uni}.

For the (30,51) and (5,30) mutants, the oxidized species co-elute with one of the single mixed-disulfide forms, so only the second mixed-disulfide form could be isolated. For these mutants, the disulfide rearrangement experiment was carried out starting from only one of the mixed-disulfide forms. Since it was not possible to measure the population of oxidized species directly, k_{uni} was estimated by measuring the decay rate of the starting material. The rate of decay of single-mixed disulfide species is equal to the sum of two rates (see Figure 4a): one representing unimolecular disulfide formation, $k_{uni}^{y \rightarrow xSSG}$, and the second representing unimolecular glutathione shuffling between the two cysteines, $k_{uni}^{y \rightarrow GSSx}$. The sum of these two unimolecular rates (k_{app}) was measured in a disulfide rearrangement experiment for short reaction times, when the population of the products is low (<15% of total) and the decay is approximately monoexponential. k_{uni} is estimated to be half of the measured value for the sum of these two unimolecular rates ($k_{uni} = k_{app}/2$).

Remarkably, the values obtained for k_{uni} differ up to 80-fold (Table 3). At pH 7.3, 25 °C, k_{uni} for (14,38) is the largest (6.5×10^{-2} s^{-1}) and the value for (5,51) is the smallest (8×10^{-4} s^{-1}). For formation of the other native disulfide bonds (i.e., those found in native BPTI), the k_{uni} values for (5,55) and (30,51) are 40- and 15-fold smaller, respectively, than k_{uni} for (14,38).

Effect of Intrinsic Reactivities on Step 2 Kinetics (k_{bi} Measurements). The differences in the k_{uni} rates described above could, in principle, result from differences in intrinsic chemical reactivities (i.e., local effects) or from the conformational properties of the polypeptide chain (i.e., non-local effects) or both. The six peptide fragments of BPTI described earlier serve as excellent models for determining local sequence effects on the intrinsic reactivities for mixed-disulfide bond formation (Table 2). These peptide fragments were also used to measure k_{bi}, the intrinsic rate of formation of a disulfide between two cysteines in fragments of BPTI.

The method for measuring k_{bi} is outlined schematically in Figure 5a. First, the glutathione mixed-disulfide form was prepared for each of the six peptides. Then the reduced form of one peptide was mixed with an excess of the mixed disulfide of a second peptide. The species formed during the disulfide rearrangement reaction (Figure 5a) were separated and quantitated using HPLC (Figure 5b).

Formation of a disulfide bond can occur with either cysteine residue acting as a nucleophile. Thus, there are two distinct rates for forming each disulfide (Szajewski & Whitesides, 1980). Both rates were measured here: first, using reduced P*x* and the mixed disulfide P*y*SSG, and second, using P*y* and P*x*SSG. Although it need not be so, we find that both rate constants for forming a given disulfide bond do not differ by more than 30%. The final k_{bi} (Table 3) is

Table 3: Effective Concentrations (C_{eff}) for Different Pairs of Cysteines in BPTI, Determined by Comparing Bimolecular Rates of Disulfide Bond Formation in Peptide Fragments (k_{bi}) to the Corresponding Unimolecular Rates in Intact Protein Mutants of BPTI (k_{uni})

	this work (pH 7.3, 25 °C)			previous studies C_{eff} (pH 8.7)[d]		
cysteine pair	k_{bi}[a] (M^{-1} s^{-1})	k_{uni}[b] (10^{-3} s^{-1})	C_{eff}[c] (mM)	**1**[e]	**2**[f]	**3**[g]
5/14	0.65	11.0	16.9			
5/30	0.35	1.5	4.3		8.5	
5/38	1.20	8.3	6.9			
5/51	0.13	0.8	6.2		2.5	
5/55	0.27	1.7	6.3	9	4.6	
14/30	1.45	5.9	4.1			
14/38	2.40	65.0	27.0	30		20
14/51	0.75	5.6	7.5			
14/55	1.40	8.8	6.3			
30/38	1.70	29.0	17.1			
30/51	0.35	4.3	12.3	30	14	
30/55	0.95	6.2	6.5			
38/51	1.10	10.5	9.5			
38/55	1.85	15.0	8.1			
51/55	0.70	10.0	14.0		10.5	
8 M urea						
5/14	0.10	1.4	14.0			
5/51	0.03	0.1	3.3		0.4	
5/55	0.05	0.3	6.0		1.0	
14/30	0.24	1.4	5.8			
14/38	0.50	3.0	6.0			<8
30/38	0.30	7.6	25.0			
30/51	0.11	0.8	7.3		3.3	

[a] Rate constants for bimolecular disulfide exchange were measured with two appropriate peptide fragments of BPTI containing one cysteine each, as described in Materials and Methods. The rate measurements are reproducible within ±10%, and the precision of concentration measurements is better than ±5%, so the accuracy of k_{bi} measurements is estimated to be ±15%. [b] Rate constants for unimolecular disulfide rearrangement were measured with the mixed-disulfide form of each BPTI mutant containing two cysteines, as described in Materials and Methods. The estimated accuracy is ±10%, based on repeated measurements of the same k_{uni} in mutants (5,55), (5,51), (14,30), and (14,38). [c] The effective concentrations of different cysteine pairs were calculated as a ratio of k_{uni} and k_{bi} (Figure 7). [d] The effective concentrations of some cysteine pairs, as measured previously, are given. [e] Creighton and Goldenberg (1984): the C_{eff} was measured at pH 8.7 in intact BPTI. [f] Darby and Creighton (1993): C_{eff} values for BPTI mutants containing only two cysteines with the other four cysteines substituted by serines, were measured at pH 8.7. [g] Goodman and Kim (1990): C_{eff} for cysteines 14 and 38 were measured in a peptide fragment of BPTI, with a sequence corresponding to residues 14 through 38.

the average of the two rate constants measured. The reduced form of peptide P30 coeluted with the mixed-disulfide form of peptide P51, so in this case, k_{bi} is the result of a single experiment. The measured values for k_{bi} differ up to 20-fold, the fastest being the rate of forming the 14-38 disulfide. These results demonstrate that one cannot simply assume a constant value for the intrinsic rate of disulfide bond formation in a protein.

Effect of Structure in the Unfolded State on Step 2 Kinetics (Effective Concentration Measurements). The kinetic effective concentration (C_{eff}) describes the impact of the polypeptide conformation on the rate of intramolecular disulfide formation. C_{eff} is defined here as the concentration of a thiol in a pseudo-first-order bimolecular reaction, yielding the observed rate of a unimolecular process between otherwise identical thiol groups (Figure 7). Thus, by definition

$$k_{bi}\,(M^{-1}\,s^{-1})C_{eff}\,(M) = k_{uni}\,(s^{-1}) \qquad (8)$$

The values for C_{eff} were calculated as a ratio of k_{uni} and k_{bi} for all possible pairs of cysteines in BPTI (Table 3 and Figure 6a). For the majority of cysteine pairs, the effective concentration is approximately 10 mM, increasing slightly with decreasing distance between cysteines (Figure 6a). Only for (14,38) is the value significantly larger (27 mM).

Disulfide rearrangement rates were also measured for some BPTI mutants in 8 M urea (Table 3). Under these conditions, the rate of bimolecular rearrangement (k_{bi}) drops approximately 5-fold. For all of the tested mutants but one, the unimolecular rate of rearrangement (k_{uni}) in 8 M urea decreases no more than 8-fold (Table 3). For (14,38), however, the decrease is 20-fold, strongly suggesting the presence of non-random structure.

DISCUSSION

Our Results. It has been postulated that the formation of the first disulfide in BPTI is essentially random (Creighton, 1985, 1988). We find, however, that the unimolecular disulfide formation rates (k_{uni}) for BPTI differ 80-fold at pH 7.3, 25 °C, and that k_{uni} for the formation of a disulfide bond between cysteines 14 and 38 is much faster than for other pairs (Table 3). Of the nine different disulfide bonds that may possibly form from mixed disulfides of Cys 14 or 38, one of them, linking cysteines 14 and 38, forms with a much greater frequency (40%) as a result of a higher k_{uni}.

There are two possible explanations for the observed variations in k_{uni}. The intrinsic reactivities of the cysteines may be different, and/or their effective concentrations may be different. The reactivities of BPTI cysteines toward mixed disulfides (k_{bi}) (Table 3), or toward glutathione or iodoacetate (Table 1), show significant differences, up to 20-fold. Thus, the influence of intrinsic cysteine reactivities on the disulfide rearrangement pathway cannot be neglected, at least in the early stages of folding, when conformational barriers are relatively low. A correlation has been observed previously between disulfide rearrangement rates and the proximity of charged amino acids to the cysteines in the sequence (Zhang & Snyder, 1988). Indeed, in BPTI, positively charged

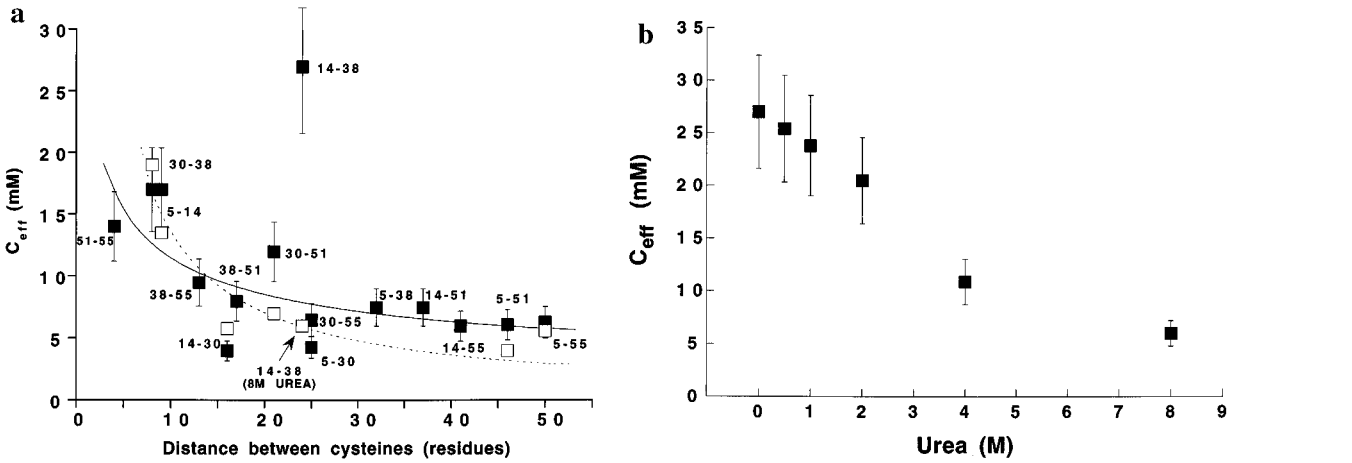

FIGURE 6: (a) Effective concentrations of different cysteine pairs in BPTI (Table 3) plotted as a function of the distance between cysteines in the sequence (filled squares). The effect of 8 M urea on some of the values is also shown (open squares). The solid line shows the best fit of equation n^{-Z} (n = the number of residues between cysteines) to the data obtained in the absence of urea, excluding (14,38). The best fit exponent is $Z = 0.5$. For the data obtained in 8 M urea, the best fit is for $Z = 1.0$ (dotted line), as compared to Z values of 2.16 (Redner, 1980) or 2.42 (Chan & Dill, 1990), expected for a random polymer. The estimated error is indicated, based on the accuracy of k_{uni} and k_{bi} measurements. (b) C_{eff} in (14,38) as a function of urea concentration.

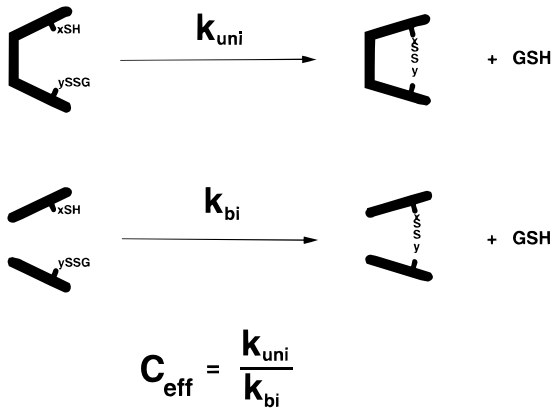

FIGURE 7: Schematic representing the difference between bimolecular and unimolecular formation of a disulfide bond. In a bimolecular process, a free thiol of a peptide rearranges with the mixed-disulfide form of a different peptide, with subsequent formation of a peptide heterodimer linked by a disulfide bond. In a unimolecular process, a free thiol group rearranges with the mixed disulfide of a different cysteine from the same molecule.

residues flank the most reactive cysteines (14 and 38) and negatively charged residues are found near slower reacting cysteines (5 and 51).

Differences in intrinsic reactivities largely account for the differences in k_{uni} among the different cysteines in BPTI. Nevertheless, the 20-fold difference in k_{bi} between the least reactive pair of thiols (5 and 51) and the most reactive pair (14 and 38) (Table 3) does not account fully for the observed 80-fold difference in k_{uni}, implying that there are significant differences in the kinetic effective concentration (C_{eff}) for the different cysteine pairs. Indeed, as shown in Figure 6a, C_{eff} for the 14-38 pair is larger than for the other pairs.

For all of the cysteine pairs but one, the kinetic C_{eff} is in the range 4−17 mM (Table 3). For these cysteine pairs, addition of up to 8 M urea does not change the C_{eff} values more than 2-fold. With or without urea, C_{eff} values for these cysteine pairs increase with decreasing distance between cysteines, but the distance dependence is weaker than expected for a randomly fluctuating polymer chain (Redner, 1980; Chan & Dill, 1990).

For cysteines 14 and 38, the effective concentration is over three-fold higher than expected on the basis of the values obtained for other pairs (Figure 6a). This difference decreases upon addition of urea (Figure 6b), suggesting that, under folding conditions, residual structure in the otherwise unfolded, reduced state brings cysteines 14 and 38 relatively close to each other. Urea presumably disrupts this structure, but the transition is broad, suggesting that residual structure in the otherwise unfolded state is stabilized in a non-cooperative manner. It is noteworthy that a synthetic variant of BPTI, containing the 14-38 disulfide bond, with the remaining cysteines replaced by α-amino-*n*-butyric acid, has been reported to form a β-sheet molten globule (Ferrer et al., 1995).

Comparison with Other Results. The average intramolecular rate of formation of the one-disulfide species in BPTI has been reported to be 3.3 s^{-1} at pH 8.7 (Creighton & Goldenberg, 1984). Each mixed disulfide in BPTI can react with five other cysteines to form a disulfide bond. Thus, if formation of the one-disulfide intermediates is a random event (at least initially), the average k_{uni} value in BPTI is predicted, on average, to be 0.66 s^{-1} at pH 8.7. The k_{uni} values for five different cysteine pairs, however, measured in a series of BPTI mutants containing only two cysteines each range from 0.006 to 0.06 s^{-1} at pH 8.7 (Darby & Creighton, 1993), at least 10-fold less than the predicted average value. None of the mutants in the series cited above contain either Cys-14 or Cys-38. The high value of k_{uni} for the 14-38 disulfide observed here, as well as the higher intrinsic reactivities of cysteines 14 and 38, provides a potential explanation for this discrepancy. It has also been observed previously that when cysteines 14 and 38 are modified or mutated in BPTI, the average rate of formation for the first disulfide decreases (Kosen et al., 1992; Creighton, 1977a), consistent with our finding that formation of the 14-38 disulfide is fast.

The reactivities of cysteines in peptide fragments toward glutathione and iodoacetate, measured here at pH 7.3 (Table 1), show larger differences (8-fold) than the 2.5-fold difference measured previously in the reaction of BPTI cysteines with iodoacetate at pH 8.7 (Creighton, 1975). At higher pH, however, the majority of cysteine side chains are negatively charged, and rate differences arising from the different p*K*s of the cysteines are thus diminished.

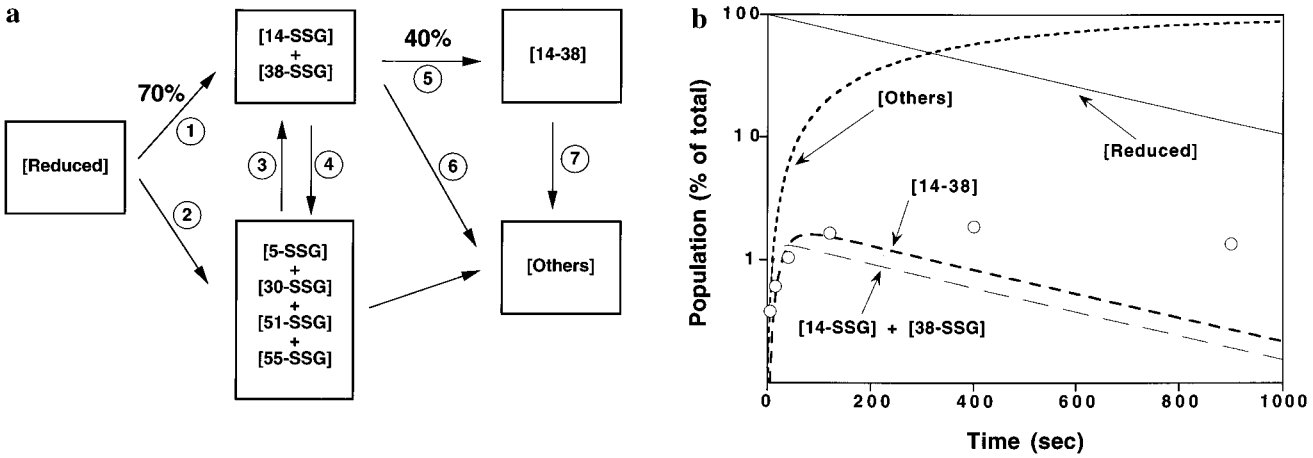

FIGURE 8: (a) Kinetic intermediates in the early stages of BPTI folding, based on the rate constants for disulfide rearrangements measured in mutants. The rate constants for mixed-disulfide formation are sums of the appropriate thiol - glutathione rate constants (4.8 and 2.4 M^{-1} s^{-1}, for steps 1 and 2, respectively; see text). The rate of disulfide formation between cysteines 14 and 38 has been measured directly (0.06 s^{-1} for step 5; Table 3). The rates of glutathione shuffling between the mixed-disulfide species and rearrangement to other unimolecular disulfides have been estimated from average values of k_{uni} between appropriate forms (0.02, 0.045, 0.045, and 0.09 s^{-1} for steps 3, 4, 6, and 7, respectively). The ratio of rates (in %) shows that in the early stages of BPTI folding, a significant flux of molecules proceed through a species containing a disulfide bond between cysteines 14 and 38. (b) Populations of different intermediates during early stages of BPTI folding, simulated using rates from Figure 8a. The population of [14-38] observed during the folding of native BPTI (Dadlez & Kim, 1995) is also shown (open circles).

The effective concentrations for some of the cysteine pairs in BPTI have been measured previously, and these results are summarized in Table 3. Our data are in qualitative agreement with these measurements, except for significant differences in the C_{eff} values for (5,30) and (5,51). Also, the decrease in the C_{eff} of cysteine pairs at high urea concentrations reported by Darby and Creighton (1993) contrasts with the weak dependence reported here. The most significant difference between our work and earlier studies of the formation of one-disulfide intermediates of BPTI is that we utilize fragments of BPTI, rather than a model thiol, as reference states. The importance of using an accurate reference state is shown by our observation that the intrinsic reactivities of BPTI cysteines with glutathione differ by 8-fold (Table 1).

Structure of Reduced BPTI. Circular dichroism and optical rotatory dispersion studies (Kosen et al., 1981; Gussakovsky & Haas, 1992; Ferrer et al., 1995) indicate that reduced BPTI is devoid of significant amounts of secondary structure. The hydrodynamic volume of reduced BPTI, as measured by electrophoretic mobility, does not depend on denaturant concentration (Creighton, 1979) or upon introduction of single amino acid substitutions (Goldenberg & Zhang, 1993). In addition, UV absorption studies (Kosen et al., 1980) show that aromatic residues in reduced BPTI are extensively solvated.

Other methods, however, detect conformational preferences and an overall collapsed structure in reduced BPTI. Fluorescence energy transfer studies (Amir & Haas, 1988; Amir et al., 1992; Gottfried & Haas, 1992; Ittah & Haas, 1995) suggest a collapsed structure. Although earlier studies of reduced BPTI and its variants did not detect significant binding of ANS (Gussakovsky & Haas, 1992; Darby & Creighton, 1993), a recent study (Ferrer et al., 1995) has found considerable binding of ANS by reduced BPTI. NMR studies of reduced BPTI (Roder, 1981; Kemmink et al., 1993), reduced BPTI models (Lumb & Kim, 1994; Pan et al., 1995), or short fragments (Kemmink et al., 1993; Kemmink & Creighton, 1993; Lumb & Kim, 1994; Staley & Kim, 1994) indicate that many resonances deviate significantly from random-coil chemical shift values. Taken together, these studies suggest a collapsed structure for reduced BPTI. Our results indicate a substantial deviation from random-coil behavior in reduced BPTI, but also indicate that the global structure of reduced BPTI does not affect the accessibility of cysteine residues appreciably.

BPTI Folding Pathway. The [14-38] intermediate, which contains one disulfide bond between residues 14 and 38, was recently detected in the early stages of BPTI folding (Dadlez & Kim, 1995). In addition, a synthetic model of the [14-38] intermediate, in which the remaining cysteines are replaced by α-amino-*n*-butyric acid, shows considerable folded structure (Ferrer et al., 1995; Barbar et al., 1995; Pan et al., 1995). The rates of formation and rearrangement of [14-38] are both very fast, suggesting that a significant fraction of BPTI molecules fold by way of the [14-38] intermediate (Dadlez & Kim, 1995).

Our results can be used to evaluate the kinetic role of [14-38] in the BPTI folding pathway, provided that we assume that the Cys→Ala mutations used in our BPTI variants are silent. In particular, knowledge of the rates for each step in the formation of each disulfide bond in unfolded BPTI permits calculation of the flux through each intermediate at the initial stage of folding. Assuming that the Cys→Ala mutations model the reduced state of BPTI, our results indicate that [14-38] should be the most frequent first disulfide formed in BPTI, accounting for 30% of the initial one-disulfide species (40% of 70% in Figure 8a). Indeed, the relative populations of [14-38], predicted using the rates measured in the Cys→Ala mutants are comparable to those observed in kinetic folding experiments with wild-type BPTI (Figure 8b). Given that the 14-38 disulfide bond is found in native BPTI, our results emphasize the importance of native-like tendencies in protein folding (Weissman & Kim, 1991; Dadlez & Kim, 1995).

ACKNOWLEDGMENT

We thank Mari Milla, Krystyna Bolewska, Mike Milhollen, Mike Burgess, and Shawn Britt for their excellent technical support. Helpful comments of Rheba Rutkowski,

Chavela Carr, Andrea Cochran, Kevin Lumb, Lorenz Mayr, Daniel Minor, and Peter Petillo on the manuscript are gratefully acknowledged.

REFERENCES

Amir, D., & Haas, E. (1988) *Biochemistry 27*, 8889−8893.

Amir, D., Krausz, S., & Haas, E. (1992) *Proteins: Struct., Funct., Genet. 13*, 162−173.

Barbar, E., Barany, G., & Woodward, C. (1995) *Biochemistry 34*, 11423−11434.

Chan, H. S., & Dill, K. A. (1990) *J. Chem. Phys. 92*, 3118−3135.

Chau, M.-H., & Nelson, J. W. (1991) *FEBS Lett. 291*, 296−298.

Creighton, T. E. (1974) *J. Mol. Biol. 87*, 563−577.

Creighton, T. E. (1975) *J. Mol. Biol. 96*, 777−782.

Creighton, T. E. (1977a) *J. Mol. Biol. 113*, 275−293.

Creighton, T. E. (1977b) *J. Mol. Biol. 113*, 313−328.

Creighton, T. E. (1979) *J. Mol. Biol. 129*, 235−264.

Creighton, T. E. (1983) *Proteins*, 1st ed., pp 321−328, W. H. Freeman and Co., New York.

Creighton, T. E. (1985) *J. Phys. Chem. 89*, 2452−2459.

Creighton, T. E. (1986) *Methods Enzymol. 131*, 83−107.

Creighton, T. E. (1988) *Biophys. Chem. 31*, 155−162.

Creighton, T. E., & Goldenberg, D. P. (1984) *J. Mol. Biol. 179*, 497−526.

Creighton, T. E., & Charles, I. G. (1987) *Cold Spring Harbor Symp. Quant. Biol. 52*, 511−519.

Dadlez, M., & Kim, P. S. (1995) *Nat. Struct. Biol. 2*, 674−679.

Darby, N. J., & Creighton, T. E. (1993) *J. Mol. Biol. 232*, 873−896.

Deisenhofer, J., & Steigemann, W. (1975) *Acta Crystallogr. B31*, 238−250.

Dobson, C. M. (1993) *Curr. Opin. Struct. Biol. 3*, 57−59.

Doering, D. S. (1992) Ph.D. Thesis, Massachusetts Institute of Technology, Cambridge, MA.

Donovan, J. W. (1969) in *Physical Principles and Techniques of Protein Chemistry, Part A* (Leach, S. J., Ed.) pp 101−170, Academic Press, New York.

Ferrer, M., Barany, G., & Woodward, C. (1995) *Nat. Struct. Biol. 2*, 211−217.

Goldenberg, D. P. (1992) *Trends. Biochem. Sci. 17*, 257−261.

Goldenberg, D. P., Bekeart, L. S., Laheru, D. A., & Zhou, J. D. (1993) *Biochemistry 32*, 2835−2844.

Goodman, E. M., & Kim, P. S. (1989) *Biochemistry 28*, 4343−4347.

Goodman, E. M., & Kim, P. S. (1990) in *Current Research in Protein Chemistry* (Villafranca, J. J., Ed.) pp 301−307, Academic Press, New York.

Gottfried, D. S., & Haas, E. (1992) *Biochemistry 31*, 12353−12362.

Gussakovsky, E. E., & Haas, E. (1992) *FEBS Lett. 308*, 146−148.

Hurle, M. R., Eads, C. D., Pearlman, D. A., Seibel, G. L., Thomason, J., Kosen, P. A., Kollman, P., Anderson, S., & Kuntz, I. D. (1992) *Protein Sci. 1*, 91−106.

Huyghues-Despointes, B. M. P., & Nelson, J. W. (1990) in *Current Research in Protein Chemistry* (Villafranca, J. J., Ed.) pp. 457−466, Academic Press, New York.

Ittah, V., & Haas, E. (1995) *Biochemistry 34*, 4493−4506.

Kemmink, J., & Creighton, T. E. (1993) *J. Mol. Biol. 234*, 861−878.

Kemmink J., van Mierlo, C. P. M., Scheek, R. M., & Creighton, T. E. (1993) *J. Mol. Biol. 230*, 312−322.

Kosen, P. A., Creighton, T. E., & Blout, E. R. (1980) *Biochemistry 19*, 4936−4944.

Kosen, P. A., Creighton, T. E., & Blout, E. R. (1981) *Biochemistry 20*, 5744−5754.

Kosen, P. A., Marks, C. B., Falick, A. M., Anderson, S., & Kuntz, I. D. (1992) *Biochemistry 31*, 5705−5717.

Kunkel, T. A., Roberts, J. D., & Zakour, R. A. (1987) *Methods Enzymol. 154*, 367−382.

Lin, T.-Y., & Kim, P. S. (1989) *Biochemistry 28*, 5282−5287.

Lumb, K. J., & Kim, P. S. (1994) *J. Mol. Biol. 236*, 412−420.

Marks, C. B., Naderi, H., Kosen, P. A., Kuntz, I. D., & Anderson, S. (1987) *Science 235*, 1370−1373.

Page, M. I., & Jencks, W. P. (1971) *Proc. Natl. Acad. Sci. U.S.A. 68*, 1678−1683.

Pan, H., Barbar, E., Barany, G., & Woodward, C. (1995) *Biochemistry 34*, 13974−13981.

Redner, J. (1980) *J. Phys. A: Math. Gen. 13*, 3526−3541.

Riddles, P. W., Blakeley, R. L., & Zerner, B. (1979) *Anal. Biochem. 94*, 75−81.

Roder, H. (1981) Ph.D. Thesis No. 6932, ETH Zürich.

Staley, J. P. (1993) Ph.D. Thesis, Massachusetts Institute of Technology, Cambridge, MA.

Staley, J. P., & Kim, P. S. (1992) *Proc. Natl. Acad. Sci. U.S.A. 89*, 1519−1523.

Staley, J. P., & Kim, P. S. (1994) *Protein Sci. 10*, 1822−1832.

Studier, F. W., Rosenberg, A. H., Dunn, J. J., & Dubendorff, J. W. (1990) *Methods Enzymol. 185*, 60−89.

Szajewski, R. P., & Whitesides, G. M. (1980) *J. Am. Chem. Soc. 102*, 2011−2026.

Weissman, J. S., & Kim, P. S. (1991) *Science 253*, 1386−1393.

Weissman, J. S., & Kim, P. S. (1992a) *Proc. Natl. Acad. Sci. U.S.A. 89*, 9900−9904.

Weissman, J. S., & Kim, P. S. (1992b) *Cell 71*, 841−851.

Weissman, J. S., & Kim, P. S. (1993) *Nature 365*, 185−188.

Weissman, J. S., & Kim, P. S. (1995) *Nat. Struct. Biol. 2*, 1123−1130.

Wlodawer, A., Nachman, J., Gilliland, G. L., Gallagher, W., & Woodward, C. (1987) *J. Mol. Biol. 198*, 469−480.

Yu, M.-H., Weissman, J. S., & Kim, P. S. (1995) *J. Mol. Biol. 249*, 388−397.

Zhang, R., & Snyder, G. H. (1988) *Biochemistry 27*, 3785−3794.

BI9616054